Direct inlet probe ion mobility spectrometry

Andriy Kuklya, Lokman Coban, Florian Uteschil, Klaus Kerpen, Ursula Telgheder

www.elsevier.com/locate/talanta

PII: S0039-9140(17)31231-6
DOI: https://doi.org/10.1016/j.talanta.2017.12.028
Reference: TAL18164

To appear in: *Talanta*

Received date: 11 November 2017
Revised date: 8 December 2017
Accepted date: 11 December 2017

Cite this article as: Andriy Kuklya, Lokman Coban, Florian Uteschil, Klaus Kerpen and Ursula Telgheder, Direct inlet probe ion mobility spectrometry, *Talanta,* https://doi.org/10.1016/j.talanta.2017.12.028

Direct inlet probe ion mobility spectrometry

*Andriy Kuklya**[1], Lokman Coban[1], Florian Uteschil[1], Klaus Kerpen[1], Ursula Telgheder[1,2]*

[1] Department of Instrumental Analytical Chemistry, University of Duisburg-Essen (UDE), Universitätsstraße 5, 45141 Essen, Germany

[2] IWW Water Centre, Moritzstr. 26, 45476 Mülheim a.d. Ruhr, Germany

Corresponding Author: * email: andriy.kuklya@uni-due.de, telephone: +49(0)201 183-6786, fax: +49(0)201 183-6773

Abstract

Direct inlet probe (DIP) was used as an introduction and a pre-separation step for atmospheric pressure photoionization time-of-flight ion mobility spectrometry (APPI-TOF-IMS) for the first time. IMS is an analytical technique used to separate and identify ionized molecules in the gas phase and under atmospheric pressure based on their mobility. The utilization of DIP prior to IMS gives the possibility to introduce the analytes into the gas phase and provides an additional separation based on their vapor pressure. The proof-of-principle study was done on example of eight polycyclic aromatic hydrocarbons (PAHs) with the ring number from 2 to 5, namely naphthalene, fluorene, anthracene, phenanthrene, pyrene, fluoranthene, benzo[a]pyrene, and benzo[k]fluoranthene. All these compounds are included in EPA priority pollutant list. Moreover, benzo[a]pyrene and benzo[k]fluoranthene are marked by EPA as probably carcinogen

compounds and also included into SCF and EU lists. To increase the sensitivity of DIP-APPI-IMS the analysis was performed using a dopant assisted ionization method (benzene, 74 mg L^{-1} in N_2). It was found that the heating rate of the interface plays a crucial role for the whole analytical procedure. To prove the ability of this method to analyze PAHs in the mixture, the mixtures containing up to five PAHs were analyzed. The LODs for the analyzed compounds obtained with DIP-APPI-IMS were found to be in the tens- or hundreds-of-microgram-per-liter range. The obtained results are promising enough to ensure the potential of DIP as an introduction and a pre-separation step for ion mobility based methods.

Graphical abstract

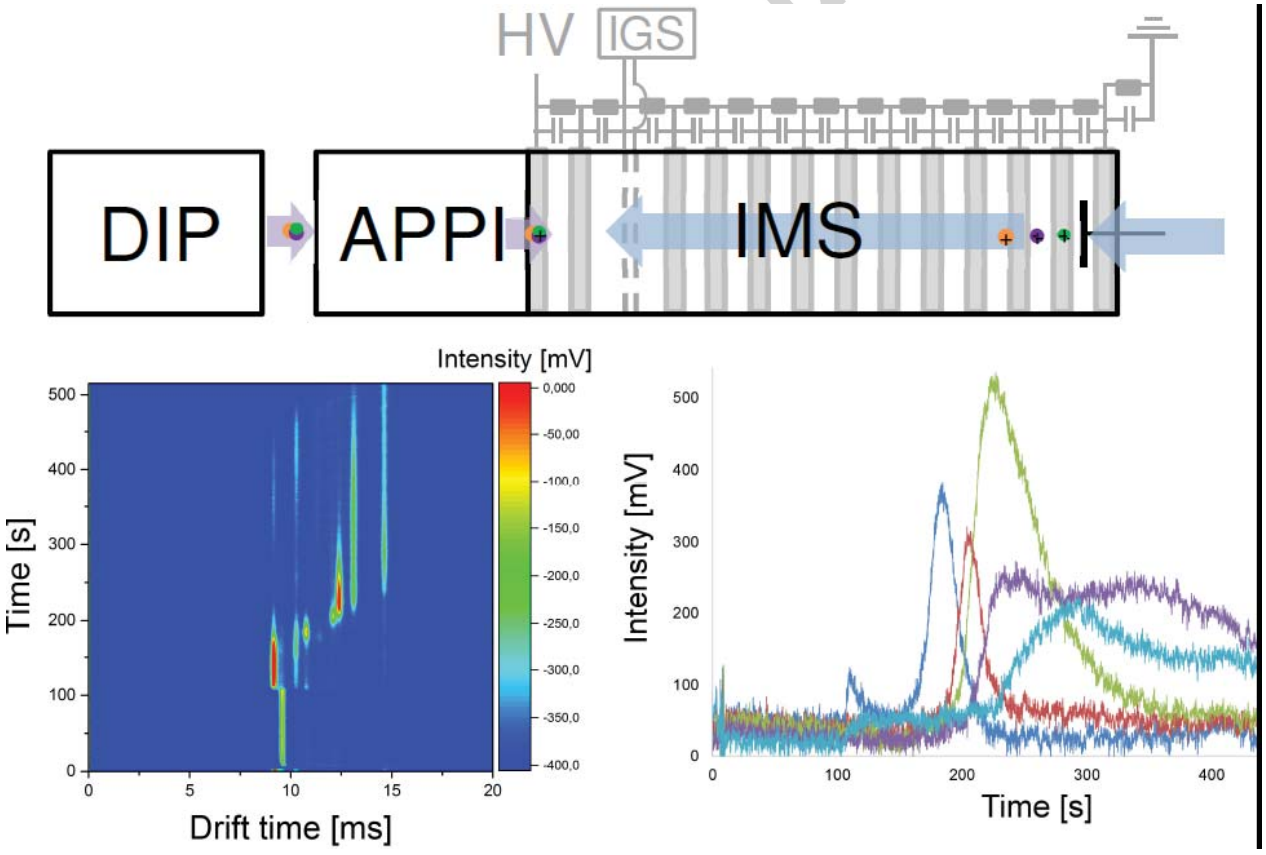

Keywords: Ion mobility spectrometry (IMS); Direct inlet probe (DIP); Polycyclic aromatic hydrocarbons (PAHs); Gas phase dopants and modifiers; On-site monitoring.

1. Introduction

Polycyclic aromatic hydrocarbons (PAHs) are nonpolar environmental pollutants that can be present in both particulate and gaseous phases. Some PAHs have been demonstrated to be carcinogenic in humans and experimental animals, and they are classified as carcinogenic materials by many organizations, including the United States Agency for Toxic Substances and Disease Registry (ATSDR), the International Agency for Research on Cancer (IARC), the Department of Health and Human Services (DHHS), the National Occupation Safety and Health Administration (OSHA), the United States Environmental Protection Agency (EPA), the European Union Scientific Committee on Food (SCF), and European Union (EU) [5,1,2,3].

Carcinogenic PAHs are found in all surface soils. The concentration of carcinogenic PAHs in forest and rural soils ranges from 5-100 μg kg^{-1} [4]. However, values of about 1000 μg kg^{-1} can be found occasionally. In metropolitan areas the concentrations of PAHs are higher as compared to those of forest and agriculture areas. The concentrations of PAHs in urban soils are usually within the range of 600-3000 μg kg^{-1}. However, levels of 8000 to 336000 μg kg^{-1} have been reported for road dust [4]. PAHs in the atmosphere are mainly collected for the analysis by two sampling models: active sampling and passive sampling. Active sampling utilizes deposition or adsorption of target PAH compounds on filters or sorbent materials. After sampling, PAHs are extracted using organic solvents such as mixtures of *n*-hexane and dichloromethane. For qualitative and quantitative analysis of extracted PAHs, gas chromatography, combined with mass spectrometry (GC-MS) or high performance liquid chromatography (HPLC), are often used

[5]. This techniques are laboratory-based and therefore require time-consuming sampling and transport procedures. Therefore, the possibility to build the analytical system as a small and transportable device gives analytical systems an additional attractiveness. The driving force for the development of miniaturized systems are the reduced cost, short analysis time, and the possibility to integrate all steps (e.g. sample preparation, separation, and detection of the analytes) in a single and portable device.

Time-of-flight ion mobility spectrometry (TOF-IMS) is the simplest and, in the same time, the most used ion mobility technique [6]. It works at atmospheric pressure and allows a direct mobility measurement. Using this technique, the complete mobility spectra can be analyzed within the time range of several tens to several hundreds of milliseconds. It was demonstrated that the resolution of 180 and 250 can be achieved with the drift tube length of 10 and 15 cm, respectively [7,8]. This technique has found many applications, e.g. detection of drugs and chemical warfare agents, quality control, determinations of contaminants in food and in environmental samples [9,10]. Over the past decades, ion mobility spectrometry has grown into an inexpensive and powerful analytical technique for the detection of gas phase samples at ambient pressure [11]. Moreover, it was demonstrated that addition of the appropriate amount of volatile organic compounds (dopant) to the sample gas can significantly enhance the sensitivity of IMS [12].

However, many of environmental pollutant have a low vapor pressure, and as a result, cannot be effectively detected by the headspace analysis. Therefore, the development of analytical methods for the detection of nonpolar compounds of limited volatility is essential.

Direct Inlet Probe (DIP) was originally developed for introduction of samples into the mass spectrometer. This technique allows fast and simple introduction of liquid and solid samples without any or with minimal sample preparation [13,14]. It is fully automatic and programmable.

It provides the temperature-programmed heating of the sample (heating rates of 0.1-3 ºC s^{-1} up to 400 ºC) resulting in time-shifted evaporation of analytes based on the difference in vapor pressures. For non-complex samples it can be considered as an alternative to the gas/liquid chromatography. In combination with mass spectrometry, this technique was used successfully for analysis of plasticizers and bisphenol A [13,15]. However, no applications of direct inlet probe and as an introduction and a pre-separation stage for ion mobility spectrometry can be found in literature.

In this work, the utilization of direct inlet probe as an introduction and pre-separation step for stand-alone ion mobility spectrometry has been introduced for the first time. Eight PAHs with the ring number from 2 to 5, namely naphthalene, fluorene, anthracene, phenanthrene, pyrene, fluoranthene, benzo[a]pyrene, and benzo[k]fluoranthene were selected as a model compounds for this study. All these compounds are included in EPA priority pollutant list. Two of selected compounds, namely benzo[a]pyrene and benzo[k]fluoranthene are marked by EPA as probably carcinogen compounds and also included into SCF and EU lists [1,2,3].

2. Experimental section

2.1 Experimental setup.

The developed in this work direct inlet probe - ion mobility spectrometer (DIP-IMS) consists of a commercially available (for different MS systems) temperature-programmed push rod (DIP) coupled to a homemade ion mobility spectrometer (IMS). The ion mobility spectrometer was equipped with atmospheric pressure photo ionization source (krypton 10.0/10.6 eV). The principle scheme and the picture of the experimental setup used in this study are shown in Figure

1 (Top) and Figure S-1, respectively. In all experiments, the drift gas and sample gas was pure nitrogen (99.999 %, Air Liquide, Germany). To introduce a dopant (benzene) in the sample gas, the sample gas flow, controlled by mass flow controller (MFC, GFC17, 0-50 mL min^{-1}, N_2), was passing through a temperature controlled vapor generator (VG; modified GC injector) equipped with a permeation tube oven. The concentration of dopant (benzene) in the carrier gas was calculated using the weight loss of the long-term stable permeation tube (PTFE, ID = 4.5 mm, OD = 6.2 mm, length = 40 mm, sealed and crimped at both ends) over a time. In the experiments presented in this work the concentration of benzene was of 74 mg L^{-1} (in N_2).

Fig. 1. Top: The principle scheme of the experimental setup. Bottom: Sample gas valve in "open" and "closed" positions.

2.2 Direct Inlet Probe (DIP).

The DIP, DIP-IMS interface, and IMS electronics were constructed by SIM GmbH (Oberhausen, Germany). The sample can be loaded into the sample vessel (volume of 10 µL) when the DIP is in load-position (see supporting information, Figure S-2). In time between the measurements, the software controlled valve is in closed-position to prevent the entering of sample into the IMS. To introduce the push rod into the interface the valve is switched to the open-position (see Figure 1, bottom). In this position the sample gas flow is directed around the push rod and the sample vessel. The temperature of the push rod tip is controlled by temperature program set in the software (Direct Inlet Probe, SIM GmbH, Oberhausen, Germany, max. 3 ramps, heating rate 0.1 to 2.0 °C s^{-1}, T_{max} = 400 °C). This enables the temperature controlled evaporation and separation of analytes according to their vapor pressures. Detailed description of working principle of DIP

can be found elsewhere [13]. The overview of the parameters and settings can be found in supporting information (see Figure S-3, right).

Valve block of DIP is connected with the IMS inlet over the stainless steel interface (ID = 7 mm, OD = 8 mm, length = 33 mm). During the analysis of the sample the tip of the push rod is positioned in the interface close to the inlet of stainless steel capillary (ID = 0.8 mm, OD = 1.6 mm, length = 25 mm). This capillary connects the interface with the entrance of the IMS ionization region (see Figure 1, bottom). In this work two different heaters was constructed to enable the heating of the interface. The first heater was the silicone mate with the maximal power of 25W (Minco Products, USA) which was rolled around the interface. The second heater was constructed from the resistance wire (0.8 m, 1 NICRO 0.5; Nikel-Chrom 80/20, D = 0.5 mm, 7 Ohm/m) and the ceramic adhesive glue (Resbond 940, Cotronics Corp, USA) directly on the outer surface of the interface (P_{max} = 30W). The outer surface of ceramic heater was isolated by about 10 mm thick glass wool.

To avoid the matrix effects, after each measurement the DIP-IMS interface was heated at 11 V (2.75 A, ~ 500 °C) for 5 min.

2.3 Ion Mobility Spectrometer (IMS).

The drift tube consists of ten cylindrical electrodes and ion gate positioned in a stack. The drift electrodes were constructed according to Gormally and Philipps [16] with an inner diameter of 25 mm, an outer diameter of 40 mm, outer thickness 5 mm, and inner thickness 1 mm. Neighbouring electrodes were insulated with spacers made out of machinable glass ceramic (Macor, O.D. 40 mm, I.D. 25 mm, and 4 mm thick). The distance between the last electrode and the detector was 5 mm. The whole length of the drift region was 104 mm. The ion mobility spectrometer was equipped with atmospheric pressure photo ionization source (DC, krypton 10.0/10.6 eV, PKS106,

Heraeus, Hanau, Germany). The distance between the photo ionization source and the first drift electrode was of 9 mm. An ion gate, designed according to Bradbury and Nielsen [17], was placed between the first and the second ring electrodes. Thus, the distance between the photo ionization source and the Bradbury and Nielsen gate (ionization region) was of 14 mm. The ion gate was made of two sets of gold-plated parallel wires (Alloy 36, 80 μm diameter) located 600 μm from each other. The wires were glued with ceramic adhesive glue (Resbond 940, Cotronics Corp, USA) between two glass ceramic rings (Macor, O.D. 40 mm, I.D. 25 mm, 4 mm thick). Transmission of ions is achieved when both wire sets have the potential corresponding to the ion shutter position in the drift tube. No significant transmission of ions can be achieved when a voltage applied to one of the wires set has a value that is at least 50 V above the voltage corresponding to the ion shutter position in the drift tube. The total period and duty cycle of the waveform were set by custom made controller unit (SIM, Germany), determining the gate pulse width and the maximal time range for the ion mobility spectrum. The drift voltage within the range of 0 to 5 kV was provided by a variable high voltage power supply (DPR 50 205 24 5 EPU, ISEQ, Germany). The detection of the ion current was carried out with a Faraday plate detector equipped with an aperture grid. The Faraday plate was made from stainless steel (9.7 mm diameter, 2 mm thickness) and connected to the input of a transimpedance amplifier (Femto DLPCA-200, Berlin, Germany). The amplifier was set to a gain of 10^{10} V A^{-1} at 7 kHz bandwidth. An aperture grid, constructed in the same way as the Bradbury Nielsen shutter, was placed at 1 mm distance in front of the Faraday plate at potential corresponding to 5% of the drift voltage. The signal was recorded with PicoScope 2205 A (Pico Technology, Cambridgeshire, UK) using PicoScope 6 software (version 6.11.12.1692).

The following IMS settings were used in this study. The Bradbury-Nielsen gate (BNG) voltage of about 50 V was required to block the ions when the ion gate is closed. The drift voltage of 4.92

kV (473 V cm^{-1}) was used to achieve fast and efficient transport of ions through the drift region of IMS. The ion gate opening time could be set between 100 and 1000 μs. In experiments demonstrated in this work, the ion gate opening time was set to 200 or 100 μs. These opening times were selected in order to achieve a good separation between the ion swarms of different analytes. The overview of the parameters and settings can be found in supporting information (see Figure S-3, left). The drift gas and sample gas flow rates were of 100 and 50 mL min^{-1}, respectively (controlled by MFCs; GFC17; 0-500 and 0-50 mL min^{-1} N_2, respectively). The overall carrier gas flow was additionally controlled by a flow meter (FM, FP-407, Applied Instruments, Netherlands) located on the exhaust of IMS.

To minimize the condensation of analytes within the IMS, the IMS drift gas temperature was kept at about 105 °C. The actual temperature of drift gas (T_h) was estimated by the following method. The drift times of selected analytes were determined firstly at 25°C (was equal to the room temperature) and then when the massive IMS aluminium heating jacket was of 106 °C. According to equation for calculation of reduced ion mobility and at constant pressure $K_0=(K_r*T_0)/T_r=(K_h*T_0)/T_h$. In this equation K_0 is a reduced mobility (mobility at standard number density, temperature [T_0, 273.15 K], and pressure [P_0, 760 torr]); T_r and T_h are room and actual temperatures, respectively; K_r and K_h are mobilities at room and at actual temperatures, respectively. Hence, $K_r/K_h=T_r/T_h$; Taking into account the relationship between mobility and drift time (t_d): $t_d=L/(K*E)$ we receive $t_{dh}/t_{dr}=T_r/T_h$; where t_{dh} and t_{dr} are drift times measured at actual and room temperatures, respectively. Thus, the actual drift gas temperature can be calculated by equation $T_h=(T_r*t_{dr})/t_{dh}$.

For each sample, three single measurements were recorded using PicoScope 6 software (version 6.11.12.1692). The settings were as follows: time range from 0 to 20 ms; intensity range from -500 to +500 mV (coupling: DC); 7813 samples pro spectra; 10 spectra pro second (10 Hz).

The data reduction was necessary for faster data analysis. Therefore, an average of 10 points was applied to reduce the number of points in a single drift spectrum from 7813 to 781 points. This resulted in much better signal-to-noise ratio with only negligible distortion in peak shape of analytes.

For the determination of peak parameters (centre, height, full width at half maximum (FWHM)), data were analyzed by the fityk (version 0.9.8) program [18]. Peaks were fitted with Gaussian functions using the Levenberg-Marquardt algorithm.

2.4 Chemicals.

To verify the proposed method eight environmentally relevant substances, namely naphthalene (Sigma-Aldrich, 99%), fluorene (Alfa Aesar, 98+ %), anthracene (Sigma Aldrich, 99%), phenanthrene (Sigma Aldrich, ≥ 99.5 %), pyrene (Sigma-Aldrich, 99%), fluoranthene (Fluka, 98.7 %), benzo[a]pyrene (Supelco, 99.9 %), and benzo[k]fluoranthene (Sigma Aldrich, ≥ 99 %), were selected. All these compounds are included in EPA priority pollutant list. Two of selected compound, namely benzo[a]pyrene and benzo[k]fluoranthene are marked by EPA as probably carcinogen compounds and also included into SCF and EU lists [3,4,5]. The empirical formulas, the molecular weights, the boiling points, and the vapor pressures of the selected for this study compounds are summarized in Table 1. The vapor pressures of the selected compounds cover a range of $1.2*10^{-5}$ to 10.4 Pa. All solutions were prepared in dichloromethane (Fisher scientific, 99.99 %). Dichloromethane has a boiling point of 39.85 °C and, therefore, can be easily evaporated prior to evaporation of the analytes. Additional advantage of dichloromethane is a high ionization potential (11.33 eV). Because this value of ionization potential is much higher than the ionization energy of Kr-photoionization source, the ionization of dichloromethane is not expected. To perform DIP-IMS analysis, 2 μL of the analyte solution was injected into the DIP

sample vessel with a Hamilton gas-tight syringe of 25 µL size, otherwise noted. To increase the sensitivity of DIP-APPI-IMS the analysis was performed using a dopant assisted ionization method with benzene as a dopant (74 mg L^{-1} in N_2). It has an ionization potential (IP) of 9.24 eV, which allows the ionization of most of aromatic compounds and was proven in our previous study to be an effective dopant for ion mobility based methods [19].Under applied experimental conditions, the drift time of the benzene peak (9.33 ms) is much shorter than the drift times of the analyzed compounds (10.86 to 14.72 ms). Therefore, the presence of benzene peak doesn't disturb quantification of analytes.

Table 1. The empirical formulas, the molecular weights, the boiling points, and the vapor pressures of the selected for this study compounds.

	EF	MW [g mol^{-1}]	BP [°C]	VP [Pa, 25°C]
Naphthalene	$C_{10}H_8$	128.17	218	10.4 [20]
Fluorene	$C_{13}H_{10}$	166.22	295	$8*10^{-2}$ [20]
Phenanthrene	$C_{14}H_{10}$	178.23	340	$1.6*10^{-2}$ [20]
Anthracene	$C_{14}H_{10}$	178.23	340	$1.1*10^{-3}$ [21]
Fluoranthene	$C_{16}H_{10}$	202.25	375	$1.2*10^{-3}$ [20]
Pyrene	$C_{16}H_{10}$	202.25	404	$6*10^{-4}$ [20]
Benzo[k]fluoranthene	$C_{20}H_{12}$	252.31	480	$2.1*10^{-5}$ [22]
Benzo[a]pyrene	$C_{20}H_{12}$	252.31	495	$1.2*10^{-5}$ [22]

3. Results and Discussion

3.1 Effect of the interface temperature on the DIP heating rate.

Interface temperature plays a crucial role in coupling of the thermal desorption units with analytical systems. Usually, the interface is kept at constant temperature that exceeds the maximal

temperature of the desorption unit. However, due to the close proximity of the DIP-IMS interface to the sample vessel the influence of the interface temperature on the temperature of the DIP sample vessel was observed (see Figure 2). When the DIP heating rate was set to 2 °C s^{-1} and the interface was not equipped with heating system the temperature gradient could be kept constant up to the temperature of about 300 °C. At higher temperature the cooling effect of stainless steel interface was strong enough to reduce the heating rate of DIP (see Figure 2, dashed line). Even higher cooling effect was observed when the interface was equipped with silicone mate heater and the heater was off. Using this setup the temperature gradient could be kept constant up to the temperature of about 280 °C. It was not possible to keep the interface at high and constant temperature because at these conditions the solvent and, partially, the analyte were evaporated from the DIP sample vessel even before the start of the temperature program. When temperature of interface was significantly higher, as compared to the boiling point of the used solvent (dichloromethane), the analyte solution was released out of the sample vessel during uncontrolled evaporation of the solvent. Therefore, the interface heating was switched off and the DIP temperature was kept at 30 °C until the complete evaporation of solvent. It was observed that a time of about 2.0 to 2.2 minutes was required for a complete solvent evaporation when the sample volume was of 2 µL (can be observed in the DIP-IMS plots, see Figures 3 and 5). After the complete evaporation of the solvent, the power supply of the interface heating system was switched on. Dependencies of DIP actual (measured) temperature on DIP set temperature (programed DIP temperature gradient was 2 °C s^{-1}) and the dependencies of interface temperature on time at different applied interface electrical power are demonstrated in Figure 2 and Figure S-4 (see supporting information), respectively. It was observed that the minimal electrical power of 15W (9V, 1,67A) is required to enable the heating of the DIP with the temperature gradient of 2 °C s^{-1} up to 400°C.

Fig. 2. The relationships between the actual (measured) and set DIP temperatures at different applied electrical power. The differences between set and actual DIP temperatures at different applied electrical power are demonstrated in insert.

3.2 Analysis of PAHs mixtures.

In addition to the DIP separation (based on the vapor pressure difference, second-to-minute time domain), IMS provide separation in the drift time (based on the cross sections of the analyte ions, millisecond time domain) which increase the discrimination ability of the analytical procedure. To prove the feasibility of DIP-APPI-IMS for the analysis of the PAHs mixtures the solution containing 0.6 mg L^{-1} of naphthalene, 0.6 mg L^{-1} of fluorene, 0.9 mg L^{-1} of anthracene, and 3.3 mg L^{-1} of pyrene was analyzed at DIP heating rates of 1 and 2 °C s^{-1}. In order to determine drift and retention times of single PAHs in the mixture, the standard solutions of PAHs were analyzed under the same conditions as the PAHs mixture. The corresponding plots (time, drift time, intensity) are demonstrated in Figure 3 (left). Relationships between the intensity of the analyte peak (at drift time maxima) and the time are demonstrated in Figure 3 (right). It was observed that the analytes are detected in order corresponding to their vapor pressures. The compounds of higher vapor pressure are detected prior to the compounds of lower vapor pressure. Moreover, it was observed that the shape of the analyte peak profile depends on the vapor pressure of the analyte. As higher the vapor pressure of the compound, as sharper the profile of the signal in the time scale (see Figure 3, right). The FWHM (in the time scale) of naphthalene, fluorene, and anthracene peaks were found to be 28, 57, and 93 s, respectively.

Fig. 3. Left: DIP-APPI-IMS plots (time, drift time, intensity) of PAHs mixture containing 0.6 mg L^{-1} of naphthalene, 0.6 mg L^{-1} of fluorene, 0.9 mg L^{-1} of anthracene, and 3.3 mg L^{-1} of pyrene. Right: Relationships between the intensity of analyte peaks (at drift time maxima) and the time. DIP heating rates were of 2 (top) and of 1 (bottom) °C s^{-1}.

Decrease of the DIP temperature gradient from 2 to 1 °C s^{-1} resulted in following changes: FWHMs (determined in time scale) of all peaks, except of pyren, were increased. The increase of FWHM for naphthalene peak (from 28 to 42 s) was much higher as compared to the increase of FWHMs for fluorene and anthracene (fluorene: from 57 to 93 s, anthracene: from 53 to 108 s). It was not possible to determine the FWHM of the pyren peak at the DIP temperature gradient of 2°C s^{-1} because of its incomplete elution. However, a shorter elution time of pyren could be achieved at the DIP temperature gradient of 1°C s^{-1}. At these conditions, the FWHM of the pyren peak was determined to be of 246 s. When the analysis was performed at DIP temperature gradient of 1 °C s^{-1}, the peaks of all analysed compounds were detected at lower temperatures as compared to those for the analysis performed at the DIP temperature gradient of 2 °C s^{-1}. It should be noted that the analysis by DIP-APPI-IMS is limited by a DIP temperature limit of 400 °C. Therefore, the detection of the signals at lower DIP temperatures is of a huge advantage because of the possibility to analyse compounds with lower vapor pressures (e.g. benzo[k]fluoranthene and benzo[a]pyrene).

The reason for the earlier detection of the analytes signals at lower DIP heating rate can be explained as follows. The temperature sensor is located not directly in the sample vessel but in its close proximity in the DIP rod. Therefore, the measured temperature may differ with the actual temperature in the sample vessel. The sample vessel is located close to the interface and therefore the exchange of thermal energy between the interface and the sample vessel can be

expected. When the interface is equipped with an external heating system the exchange of thermal energy between the interface and the sample vessel can be regulated by the input of interface electrical power. Within the first 90 s and at electrical power input of 22.5 W (11 V * 2.05 A) the heating rate of the interface is about 1.3 °C s^{-1}, which is then decreased to about 1.0 °C s^{-1} (last 90 s, see Figure S-4). The initial interface heating rate is higher than 1 °C s^{-1} and lower than 2 °C s^{-1}. Therefore, the heating of the interface results in an additional heating of the sample vessel when the DIP heating rate is slower (e.g. 1 °C s^{-1}) than the heating rate of the interface. The cooling effect is achieved when the DIP heating rate is faster (e.g. 2°C s^{-1}) than that of the interface. Ideally, the heating rate of the interface should be synchronized with that of the DIP.

Relationships between the intensity of analytes peaks and DIP temperature at DIP temperature gradients of 2 and 1 °C s^{-1} are demonstrated in Figure 4. In these plots the advantage of lower DIP temperature gradient is evident. It was observed that FWHMs (determined in temperature scale) for peaks of naphthalene, fluorene, and anthracene were reduced. The effect was especially significant for the peaks of fluorene and anthracene, which FWHMs were reduced in about two times (see Figure 4).

Fig. 4. Relationships between the intensity of analyte peaks (at drift time maxima) and the temperature for the PAHs mixture containing 0.6 mg L^{-1} of naphthalene, 0.6 mg L^{-1} of fluorene, 0.9 mg L^{-1} of anthracene, and 3.3 mg L^{-1} of pyrene. DIP heating rates were of 2 (top) and of 1 (bottom) °C s^{-1}.

The resolution in the drift time scale can be increased, at the cost of lower intensity, by reduction of the BNG gating time. The plots recorded with BNG gating time of 200 and 100 μs (DIP

temperature gradient of 1 °C s^{-1}) together with the corresponding drift spectra are demonstrated in Figure S-5 in supporting information.

3.3 Effect of the DIP overheating

To check the effect of further increase of interface temperature gradient a new heating system was constructed from the resistance wire and the ceramic adhesive glue directly on the outer surface of the interface. Despite the similar maximal power of both heating systems (25 W for silicone mate and 30 W for ceramic heating system), the ceramic heater has demonstrated higher interface heating rates as compared to that achieved with the silicone mate (see Figure S-4 and Figure S-6 in supporting information). Within the first 90 s and at electrical power input of 19.7 W (9 V * 2.19 A) the interface heating rate of about 2.4 °C s^{-1} was achieved. This heating rate is almost in two times higher as compared to the heating rate that was achieved in the previous experiments at higher electrical power input (22.5 W, 1.3 °C s^{-1}) with the silicone mate heating system. The probable reason is better heat transfer from ceramic heater to the interface. Because the ceramic heater was produced directly on the surface of the interface the heat transfer should be much better as compared to that provided by rolled around interface silicone mate. Furthermore, the material used for ceramic interface heater can be heated up to 1100 °C. This temperature limit is much higher as compared to maximal working temperature suggested for silicon mate (235 °C). Increase of the electrical power to 24.5 W resulted in increase of the initial heating rate to 2.8 °C. The further increase of the electrical power was not used in this work because the glass wool used for thermal isolation of the interface became sticky (possible melting of glass wool on surface of interface heater).

To check the performance of DIP-APPI-IMS with a new heating system a mixture of five PAHs (0.29 mg L^{-1} of naphthalene, 0.29 mg L^{-1} of fluorene, 0.88 mg L^{-1} of anthracene, 1.18 mg L^{-1} of

pyrene, and 5.3 mg L^{-1} of benzo[a]pyren) was analyzed (see Figure 5, top). Dependencies of the analyte peaks intensity (at drift time maxima) and DIP temperature (set and actual) on time are demonstrated in Figure 5 (bottom). When the DIP heating rate was set to 1 °C s^{-1} and the interface heat power was 24.5 W, the DIP temperature gradient could not be kept constant. Due to the additional heating caused by the interface the DIP heating rate was significantly increased during the first 150 s of the DIP heating program (time between 150 and 300 s). This resulted in a heating rate of about 1.46 °C s^{-1}. Within this time range an evaporation of naphthalene, fluorene, and anthracene was achieved. Due to the higher heating rate, FWHMs of naphthalene and anthracene were reduced in about 1.5-3 times (naphthalene: from 42 to 28 s; fluorene: from 93 to 26 s; anthracene from 108 to 53 s). Furthermore, the retention times (maximum in time scale) of all analytes was reduced (see Table 2). Due to earlier evaporation of the substances, the analysis of compounds of low vapor pressure (e.g. benzo[k]fluoranthene and benzo[a]pyrene) was possible. However, within the time range of 300 to 450 s the heating gradient was significantly reduced resulting in the broadening of pyren and benzo[a]pyren peaks. The results of the analysis of different PAHs mixture containing four PAHs is presented in Figure S-7. This mixture contains naphthalene (0.3 mg L^{-1}) together with the substances which were not included in the five PAHs mixture, namely phenanthrene (0.5 mg L^{-1}), fluoranthene (1.0 mg L^{-1}), and benzo[k]fluoranthene (5.0 mg L^{-1}).

Fig. 5. Top: DIP-APPI-IMS plots (time, drift time, intensity) of PAHs mixture containing 0.6 mg L^{-1} of naphthalene, 0.6 mg L^{-1} of fluorene, 0.9 mg L^{-1} of anthracene, and 3.3 mg L^{-1} of pyrene. Bottom: Relationships between the intensity of analyte peaks (at drift time maxima) and the time. DIP heating rates were of 1 °C s^{-1}.

3.4 Determination of analytical parameters for selected compounds analyzed by DIP-APPI-IMS.

In order to prove the effectiveness of DIP-APPI-IMS eight selected compounds were analyzed by DIP-APPI-IMS using both (the silicone mate and the ceramic) heating systems. The DIP-temperature gradient was of 2 and 1 °C s^{-1} for silicone mate heating system and 1 °C s^{-1} for the ceramic heating system. The injection volume was of 2µL and the time for solvent evaporation was 2.2 min. Detailed description of the IMS and DIP parameter as well as the description of the analysis method can be found in sections 2.2 and 2.3. The achieved drift times, retention times, and limits of detection (S/N = 3) are summarized in Table 2. A non-linear relationship between the signal area and the concentration, common for dopant assisted APPI, was observed for all analysed compounds. Representative DIP chromatograms and corresponding ion mobility spectra of naphthalene analysed within the concentrations range of 0 to 500 $ppb_{m/m}$ (concentration in the analyzed solution) are exemplarily presented in Figure 6.

Fig. 6. DIP chromatograms (top) and corresponding ion mobility spectra (bottom) of naphthalene analyzed within the concentrations range of 0 to 500 µg L^{-1} (concentration in the analyzed solution). The DIP-temperature gradient was of 2 °C s^{-1}, the injection volume was of 2 µL, and the time for solvent evaporation was 2.2 min.

Table 2. Drift times (DT), retention times (RT, at maximum of peak intensity), and limits of detection (LOD) for the model compounds analyzed with the silicone mate heater. RTs and LODs achieved with the ceramic heating system are demonstrated in the brackets.

	DT [ms]	RT [s, 2 °C s^{-1}]	RT [s, 1 °C s^{-1}]	LOD [µg L^{-1}]
Naphthalene	10.86	183	198 (182)	42 (34)
Fluorene	12.19	216	241 (204)	38 (36)
Phenanthrene	12.43	248	278 (222)	87 (67)

Anthracene	12.45	257	290 (227)	112 (71)
Fluoranthene	13.25	282	328 (264)	164 (128)
Pyrene	13.19	304	364 (244)	262 (173)
Benzo[k]fluoranthene	14.89	-	- (275)	- (760)
Benzo[a]pyrene	14.72	-	- (285)	- (863)

Compounds of higher vapor pressure were detected at shorter retention times as compared to compounds of lower vapor pressure. Shorter retention times were achieved with the ceramic heating system as compared to those achieved with the silicon mate heating system. The drift times have shown no significant dependence on the DIP heating rate and on the type of the heating system. The LODs of the analyzed compounds obtained with DIP-APPI-IMS were found to be in the hundreds- or tens-of-microgram-per-liter range. Compounds of higher vapor pressure demonstrate lower LODs as compared to those for the compounds of lower vapor pressure. The reason for this effect is a difference in the FWHM (determined in time scale) of analyte peaks. As mentioned in chapter 3.2, the peaks of compounds of higher vapor pressure have significantly lower FWHMs as compared to those for the compounds of low vapor pressure. Thus, the peaks of the compounds of low vapor pressure are broad (high FWHM) and the intensity is low as compared to those for the compounds of higher vapor pressure. The interface heating rate of the current heating system was found to be not constant (see Figure S-4). The heating rate decreases from the initial 1.3 °C s^{-1} to about 1.0 °C s^{-1} in the end of the analysis. This results in peak broadening for the compounds with longer retention times. Therefore, the LODs for the compounds of low vapor pressure can be potentially significantly reduced by usage of heating system with constant and sufficiently high interface heating gradient.

The normalized drift spectra of all compounds analyzed in this study are presented in Figure 7. At the applied conditions the FWHMs of all compounds were found to be within the range of 0.25 to

0.28 ms. These values correspond to a resolving power, calculated as a ratio between the drift time and FWHM, of 45-60. The resolving power can be increased, at the cost of lower intensity, by reduction of the BNG gating time. The use of faster amplifier may be another possibility to improve the resolving power. The smallest FWHM was achieved for the naphthalene peak (0.25 ms). However, with the increase of the peak drift time the values of FWHM were slightly increased. A good separation between the compounds containing two, three, four, and five rings can be achieved (see Figure 7). However, the separation between the compounds containing the same number of the cycles is rather poor. Nevertheless, the possibility to have this additional (to DIP) separation improves the overall separation ability of the DIP-APPI-IMS system.

Fig. 7. Normalized drift spectra of naphthale, fluorene, phenanthrene, anthracene, pyrene, fluoranthene, benzo[a]pyrene, and benzo[a]fluoranthene

4. Conclusion

The direct inlet probe has been found to be a suitable introduction and pre-separation step for time-of-flight ion mobility spectrometry. An attractive feature of the direct inlet probe is the fast and simple introduction of liquid and, potentially, solid samples without any or with minimal sample preparation. For non-complex samples it can be considered as an alternative to the gas/liquid chromatography. In addition to DIP separation, which is based on the differences in the vapor pressure, IMS provides separation based on the different mobilities of ions under an electric field. Combination of these two separation techniques significantly enhance the differentiation ability of ion mobility spectrometry.

In this proof-of-principle study eight polycyclic aromatic hydrocarbons (naphthalene, fluorene, anthracene, phenanthrene, pyrene, fluoranthene, benzo[a]pyrene, and benzo[k]fluoranthene),

which are included in EPA priority pollutant list, were analyzed with DIP-APPI-IMS using a dopant assisted ionization method. The LODs for these compounds were found to be in the tens- or hundreds-of-microgram-per-liter range. Further improvements and optimization may significantly increase the sensitivity and resolving power of DIP-APPI-IMS. The obtained results are promising enough to ensure the potential of DIP as an introduction and a pre-separation step for ion mobility based methods.

Acknowledgments

The authors thank Scientific Instruments Manufacturer GmbH (SIM GmbH, Oberhausen, Germany) for providing the direct inlet probe (DIP) as well as for construction of DIP-IMS interface and IMS electronics.

This work was financially supported by Bundesministerium für Wirtschaft und Energie (BMWi; ZIM Project No. KF2210322RE4).

Appendix A. Supporting information

Supplementary data associated with this article can be found in the online version at

References

[1] Office of the Federal Registration (OFR) Appendix A: priority pollutants. Fed Reg. 1982;47:52309.

[2] Scientific Opinion of the Panel on Contaminants in the Food Chain on a request from the

European Commission on Polycyclic Aromatic Hydrocarbons in Food. The EFSA Journal (2008) 724, 1-114.

[3] D. Lerda, Polycyclic Aromatic Hydrocarbons (PAHs). Factsheet. 4th edition, 2011, JRC 66955 - Joint Research Centre - Institute for Reference Materials and Measurements

[4] C.A. Menzie, B.B. Potocki, J. Santodonato, Exposure to carcinogenic PAHs in the environment, Environ. Sci. Technol., 26 (1992) 1278–1284, http://dx.doi.org/10.1021/es00031a002

[5] B.-K. Lee, V.T. Vu. Sources, Distribution and Toxicity of Polycyclic Aromatic Hydrocarbons (PAHs) in Particulate Matter, Intech, 2010. http://dx.doi.org/10.5772/10045

[6] G.A. Eiceman, Z. Karpas, H.H. Hill Jr., Ion Mobility Spectrometry, Third Edition, CRC Press, 2014.

[7] A.T. Kirk, M. Allers, P. Cochems, J. Langejuergen, S. Zimmermann, A compact high resolution ion mobility spectrometer for fast trace gas analysis. Analyst 138 (2013) 5200-5207. http://dx.doi.org/10.1039/c3an00231d

[8] A.T. Kirk, S. Zimmermann, Pushing a compact 15 cm long ultra-high resolution drift tube ion mobility spectrometer with R = 250 to R = 425 using peak deconvolution. Int. J. Ion Mobil. Spec. 18 (2015) 17-22. http://dx.doi.org/10.1007/s12127-015-0166-z

[9] H. Borsdorf, G.A. Eiceman. Ion mobility spectrometry: Principles and applications. Appl. Spectrosc. Rev. 41 (2006) 323-375. http://dx.doi.org/10.1080/05704920600663469

[10] S. Armenta, M. Alcala, M. Blanco, A review of recent, unconventional applications of ion mobility spectrometry (IMS). Anal. Chim. Acta; 703(2011) 114-123. http://dx.doi.org/10.1016/j.aca.2011.07.021

[11] R. Cumeras, E. Figueras, C.E. Davis, J.I. Baumbach, I. Gràcia, Review on Ion Mobility Spectrometry. Part 1: Current Instrumentation, Analyst. 140 (2015) 1376-1390. http://dx.doi.org/10.1039/c4an01100g

[12] E. Waraksa, U. Perycz, J. Namieśnik, M. Sillanpää, T. Dymerski, M. Wójtowicz, J. Puton, Dopants and gas modifiers in ion mobility spectrometry, Trends Analyt. Chem. 82 (2016) 237-249. http://dx.doi.org/10.1016/j.trac.2016.06.009

[13] S. Krieger, A. von Trotha, K.S.-Y. Leung, Oliver J. Schmitz, Development, optimization, and use of an APCI source with temperature-controlled vaporization of solid and liquid samples, Anal. Bioanal. Chem. 405 (2013) 1373-1381. http://dx.doi.org/10.1007/s00216-012-6531-4

[14] S. Krieger, Schmitz, Non-destructive plasticizer screening using a direct inlet probe-atmospheric pressure chemical ionization source and ion trap mass spectrometry, Rapid Commun. Mass Spectrom. 28 (2014) 1862-1870. http://dx.doi.org/10.1002/rcm.6972

[15] S. Horst, O.J. Schmitz, Quantitative Analysis of Bisphenol A in Recycled Paper with a Novel Direct Inlet Probe-Atmospheric Pressure Photoionization–IonTrap-MS, J. Anal. Test. 1 (2017) 255–263. https://doi.org/10.1007/s41664-017-0034-4

[16] J. Gormally, J. Phillips, The performance of an ion mobility spectrometer for use with laser ionization. Int. J. Mass Spectrom. Ion Processes 107 (1991) 441-451. http://dx.doi.org/10.1016/0168-1176(91)80040-T

[17] N.E. Bradbury, R.A. Nielsen, Absolute Values of the Electron Mobility in Hydrogen, Phys. Rev. 49(1936) 388-393. http://dx.doi.org/10.1103/PhysRev.49.388

[18] M. Wojdyr, Fityk: a general-purpose peak fitting program, J. Appl. Cryst. 43 (2010) 1126-1128. http://dx.doi.org/10.1107/S0021889810030499

[19] A. Kuklya, S. Joksimoski, K. Kerpen, F. Uteschil, R. Marks, U. Telgheder, Analysis of gasoline contaminated water samples by means of dopant-assisted atmospheric pressure photoionization differential ion mobility spectrometry, Int. J. Ion Mobil. Spec. 2016; https://doi.org/10.1007/s12127-016-0194-3

[20] W.J. Sonnefeld, W.H. Zoller, W.E. May, Dynamic coupled-column liquid-chromatographic determination of ambient-temperature vapor pressures of polynuclear aromatic hydrocarbons, Anal. Chem. 55 (1983) 275-280. http://dx.doi.org/10.1021/ac00253a022

[21] B.F. Rordorf, Thermodynamic and thermal properties of polychlorinated compounds: The vapor pressures and flow tube kinetics of ten dibenzo-para-dioxines, Chemosphere 14 (1985) 885-892. https://doi.org/10.1016/0045-6535(85)90209-7

[22] H. Yamasaki, K. Kuwata, Y. Kuge, Determination of Vapor Pressure of Polycyclic Aromatic Hydrocarbons in the Supercooled Liquid Phase and Their Adsorption on Airborne Particulate Matter, Nippon Kagaka Kaish. 8 (1984) 1324-1329. http://doi.org/10.1246/nikkashi.1984.1324

Highlights

- DIP is used as introduction and pre-separation step for IMS for the first time.
- The proof-of-principle study was done on example of eight PAHs.
- LOD values are in the tens- or hundreds-of-microgram-per-liter range.
- Combination of DIP and IMS significantly enhance the IMS differentiation ability.

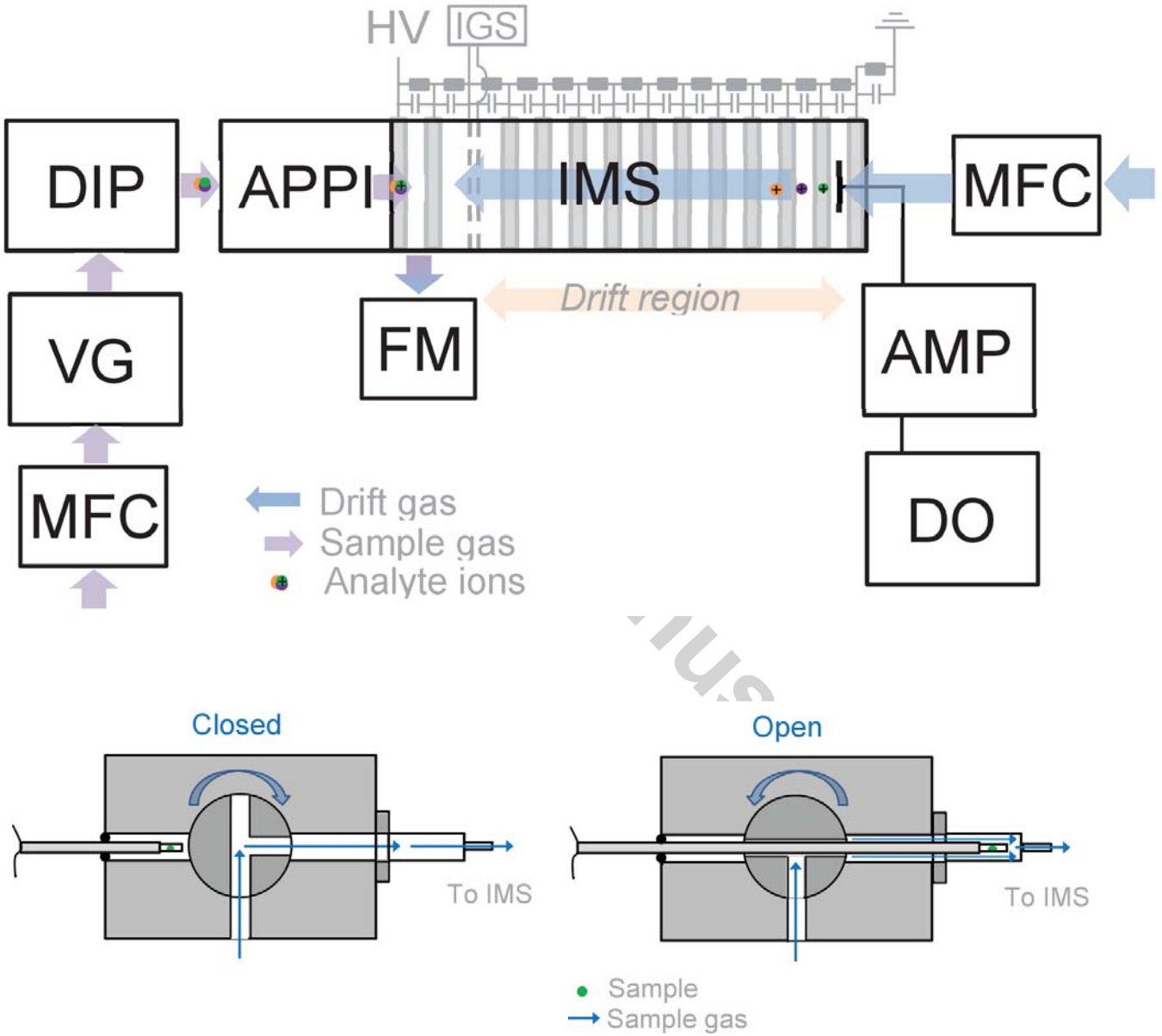

Figure 2

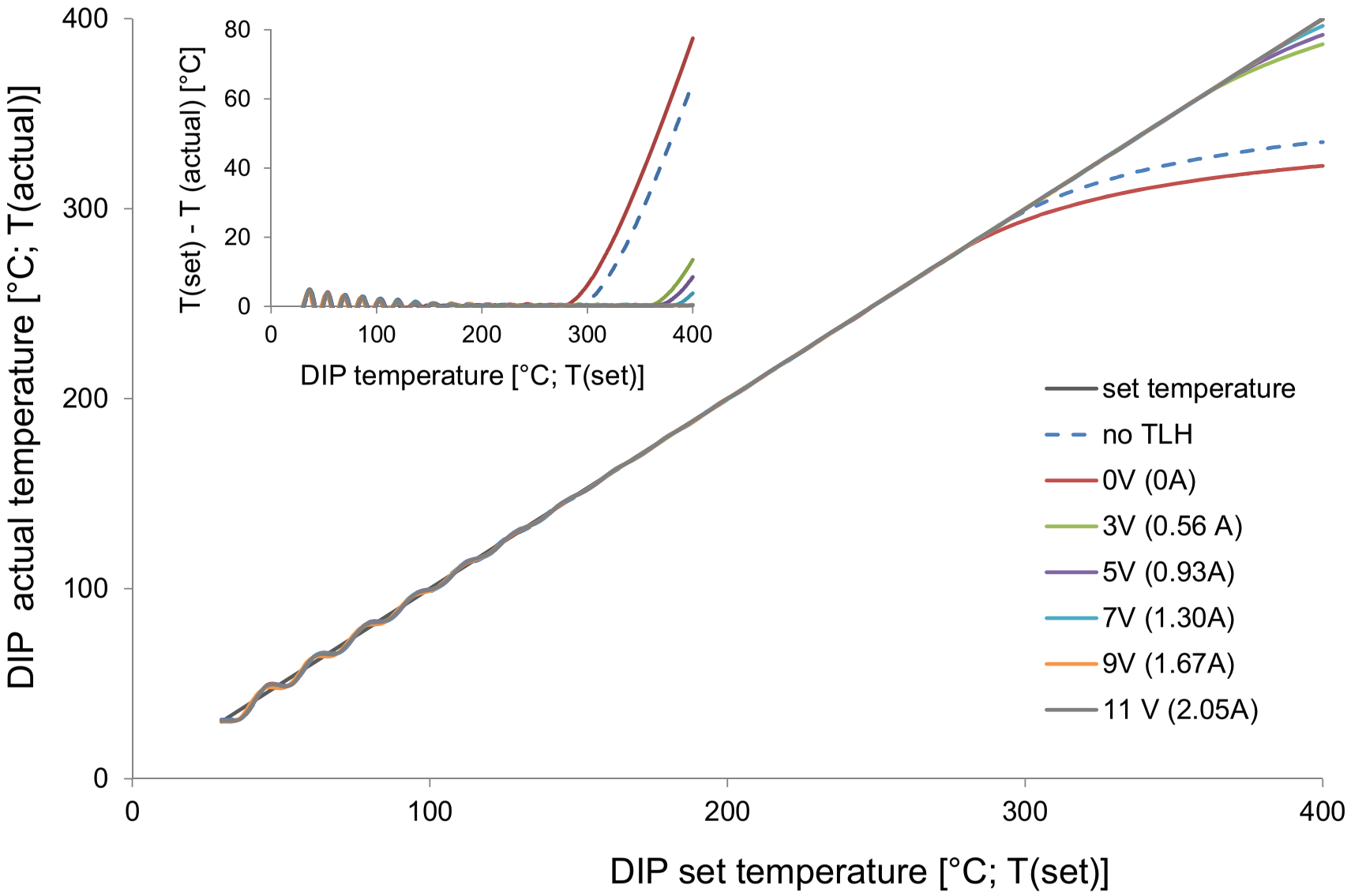

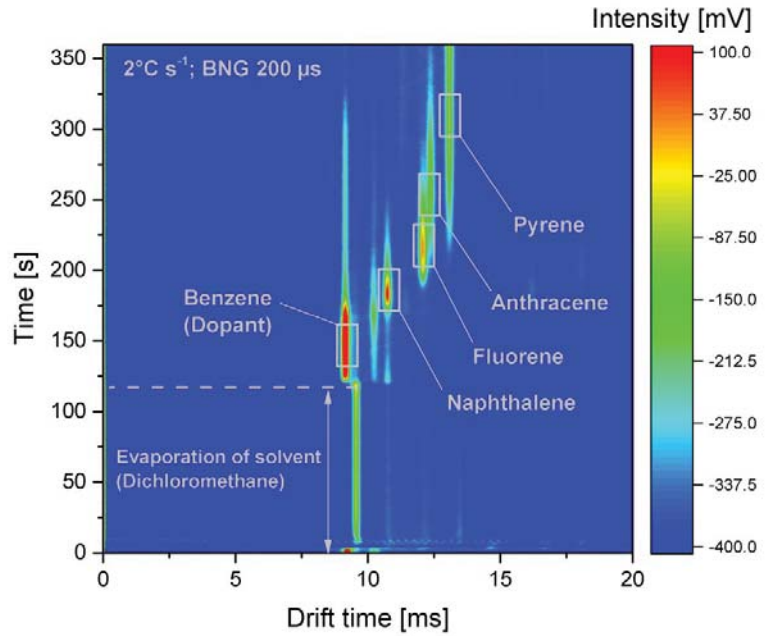

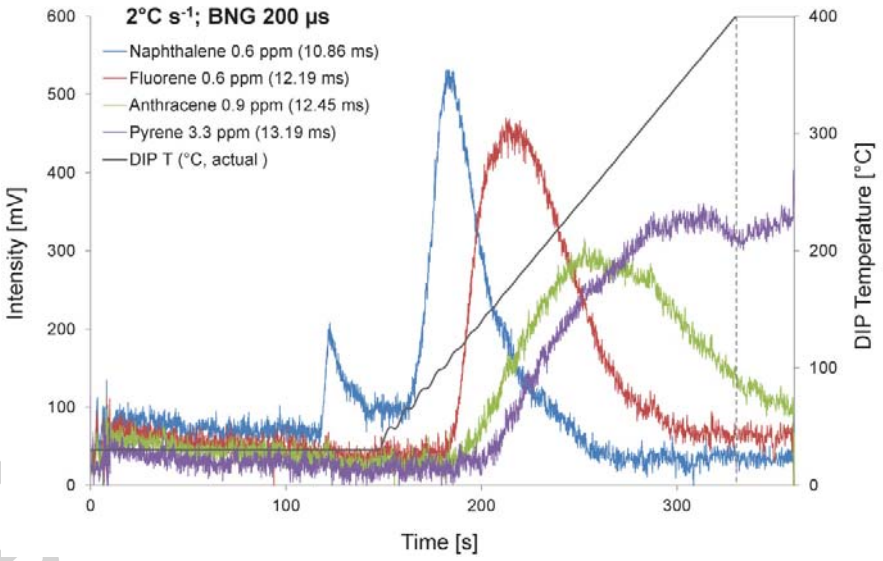

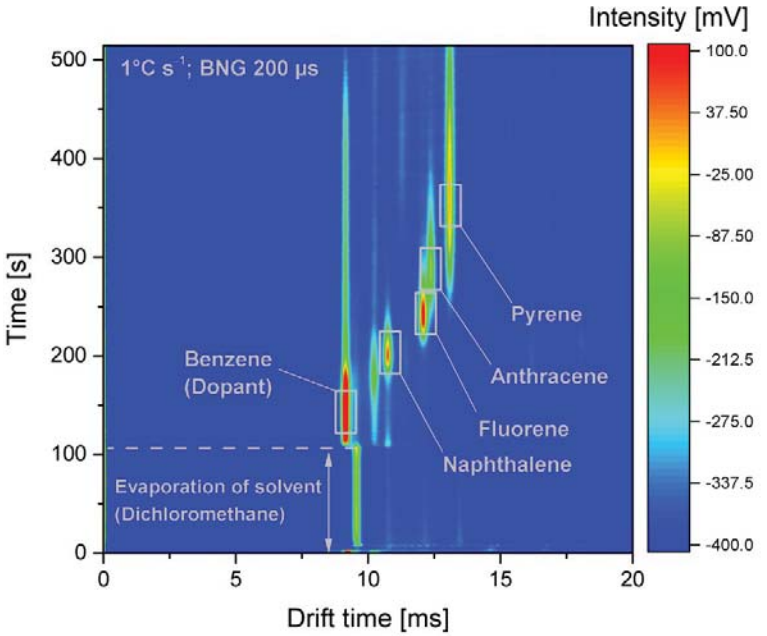

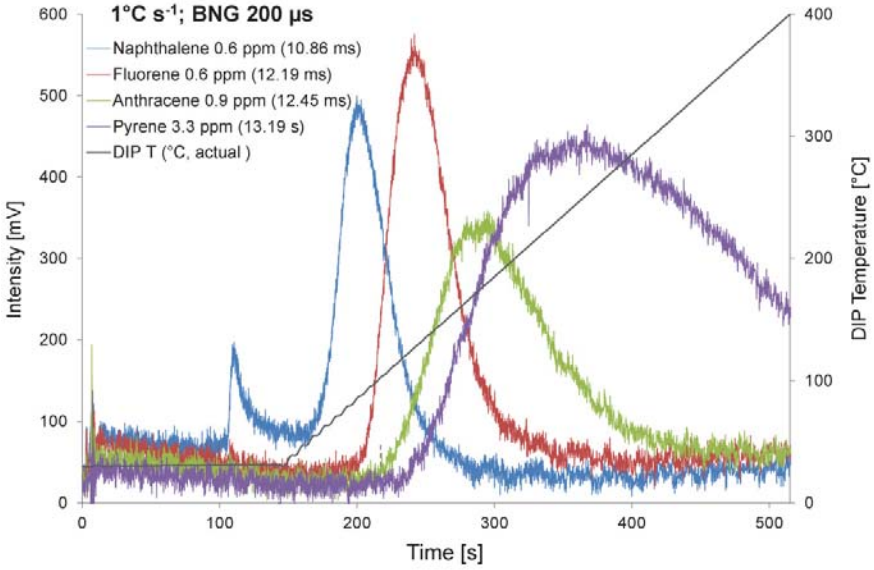

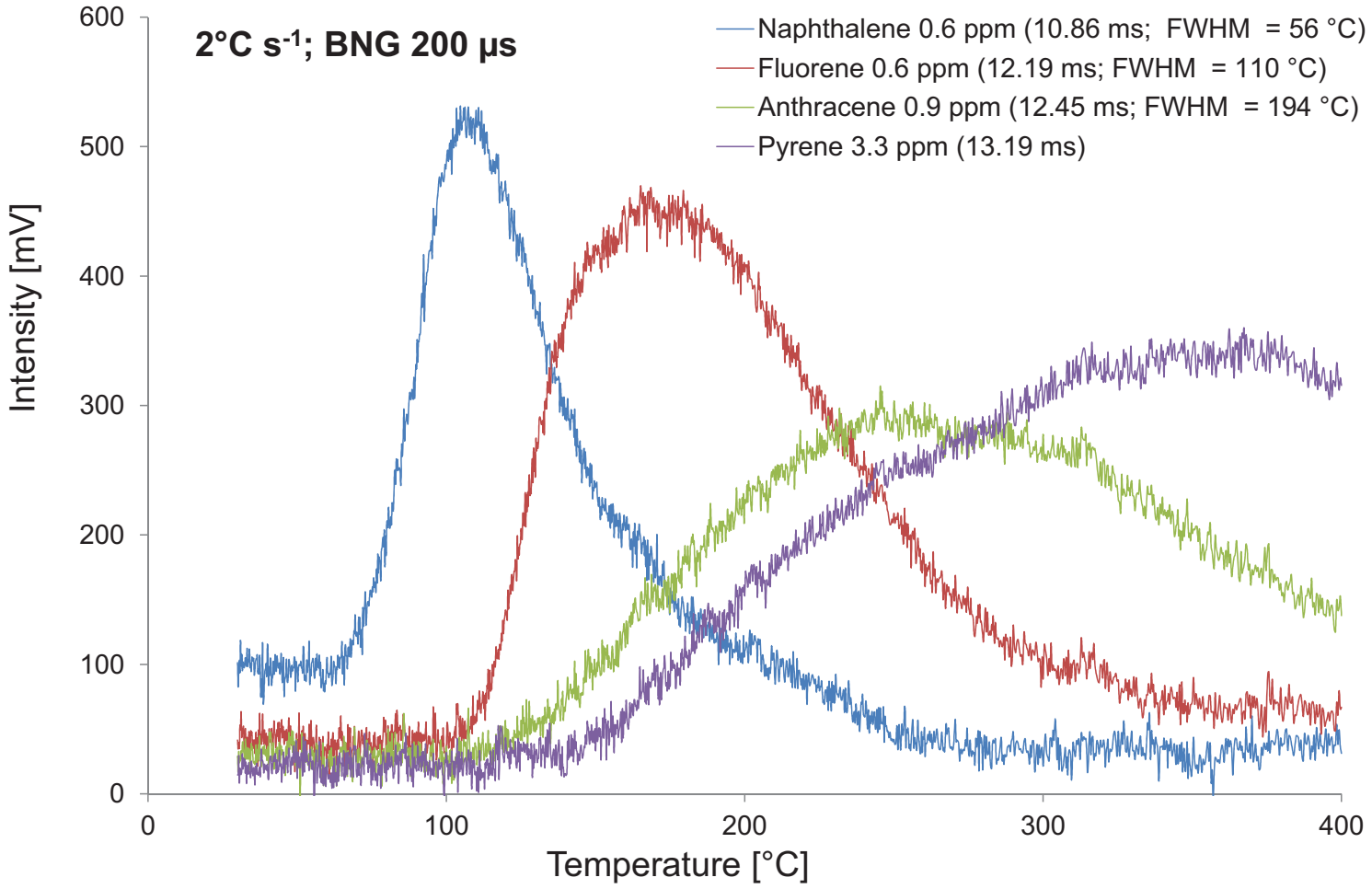

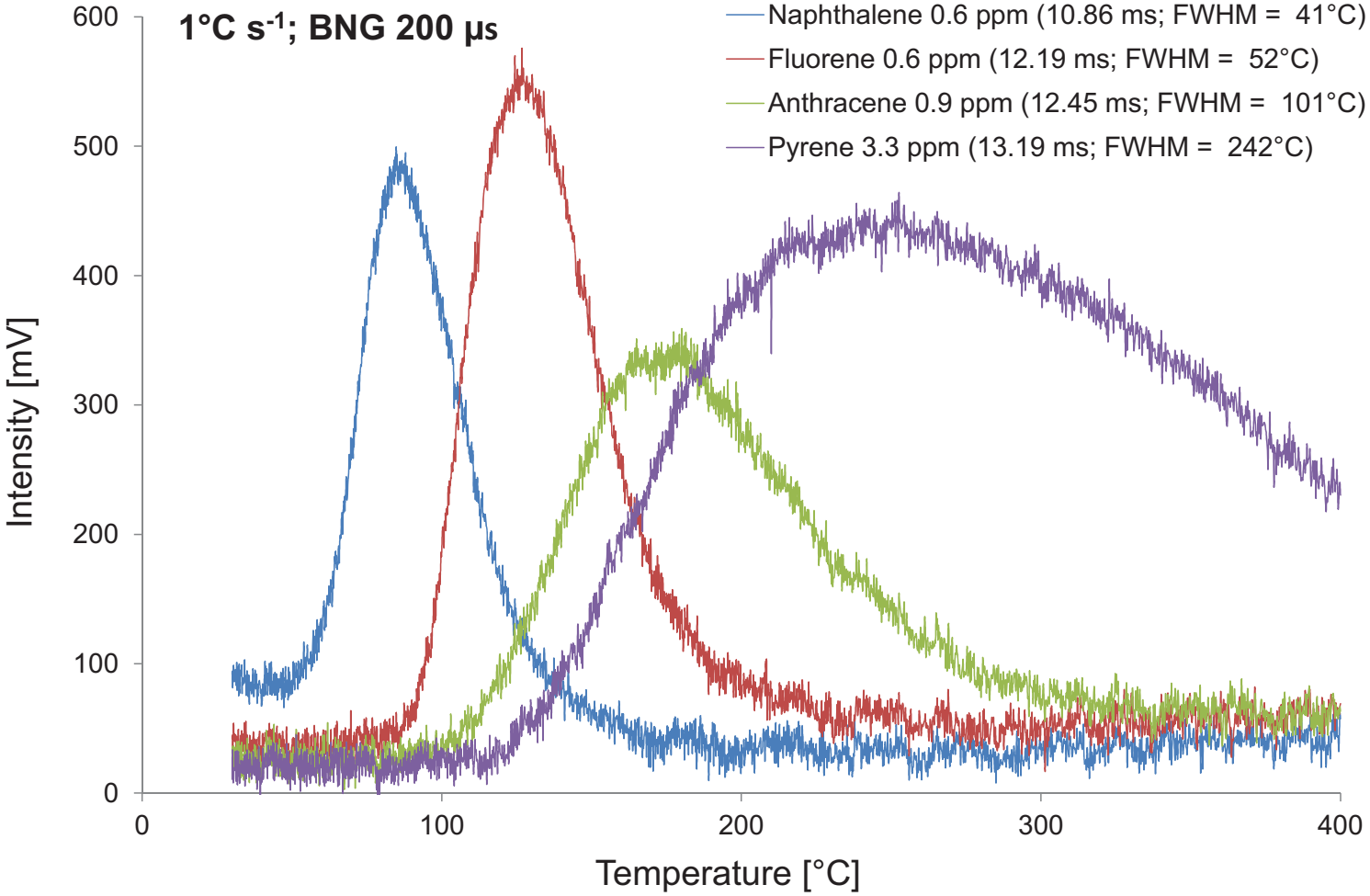

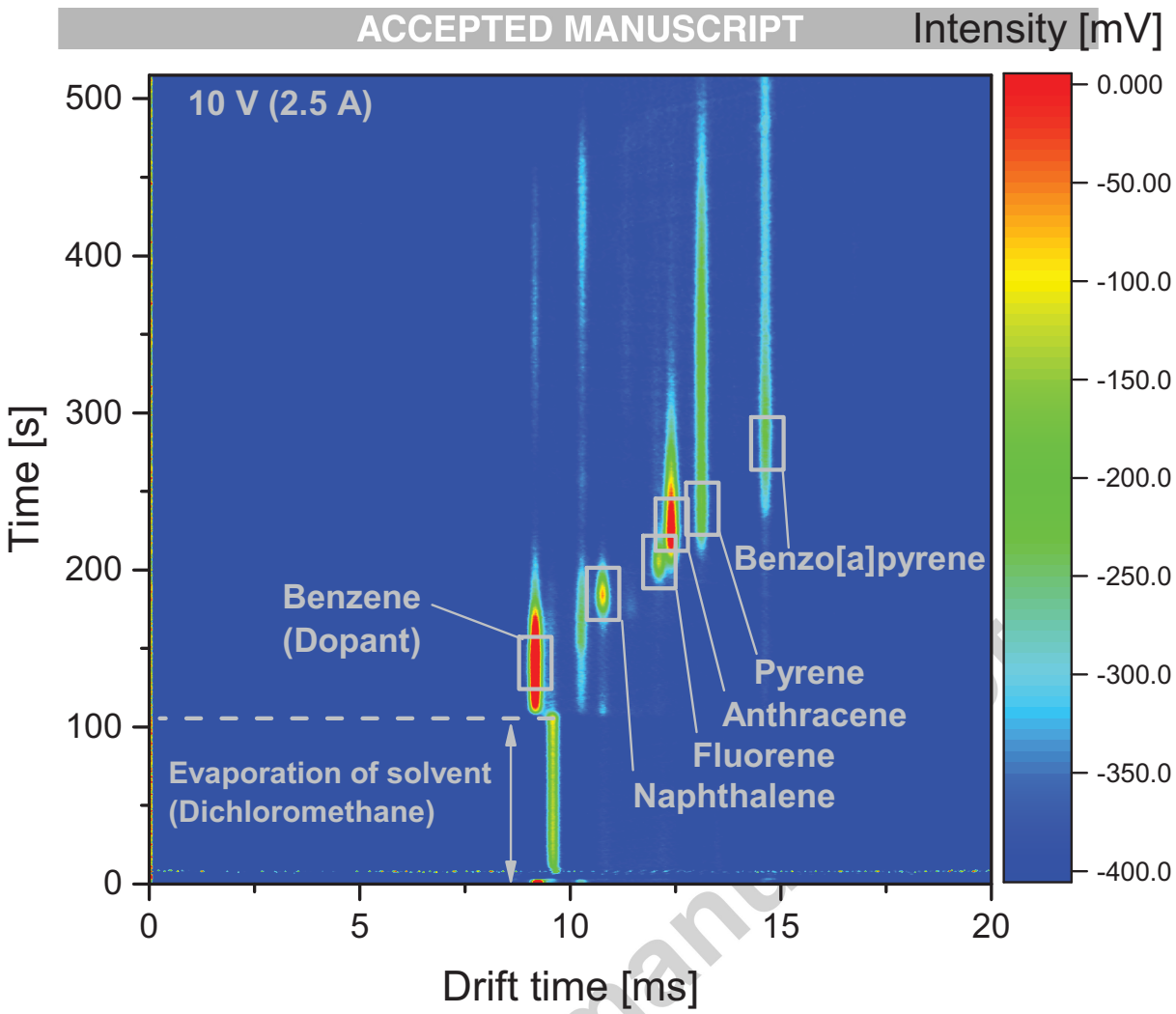

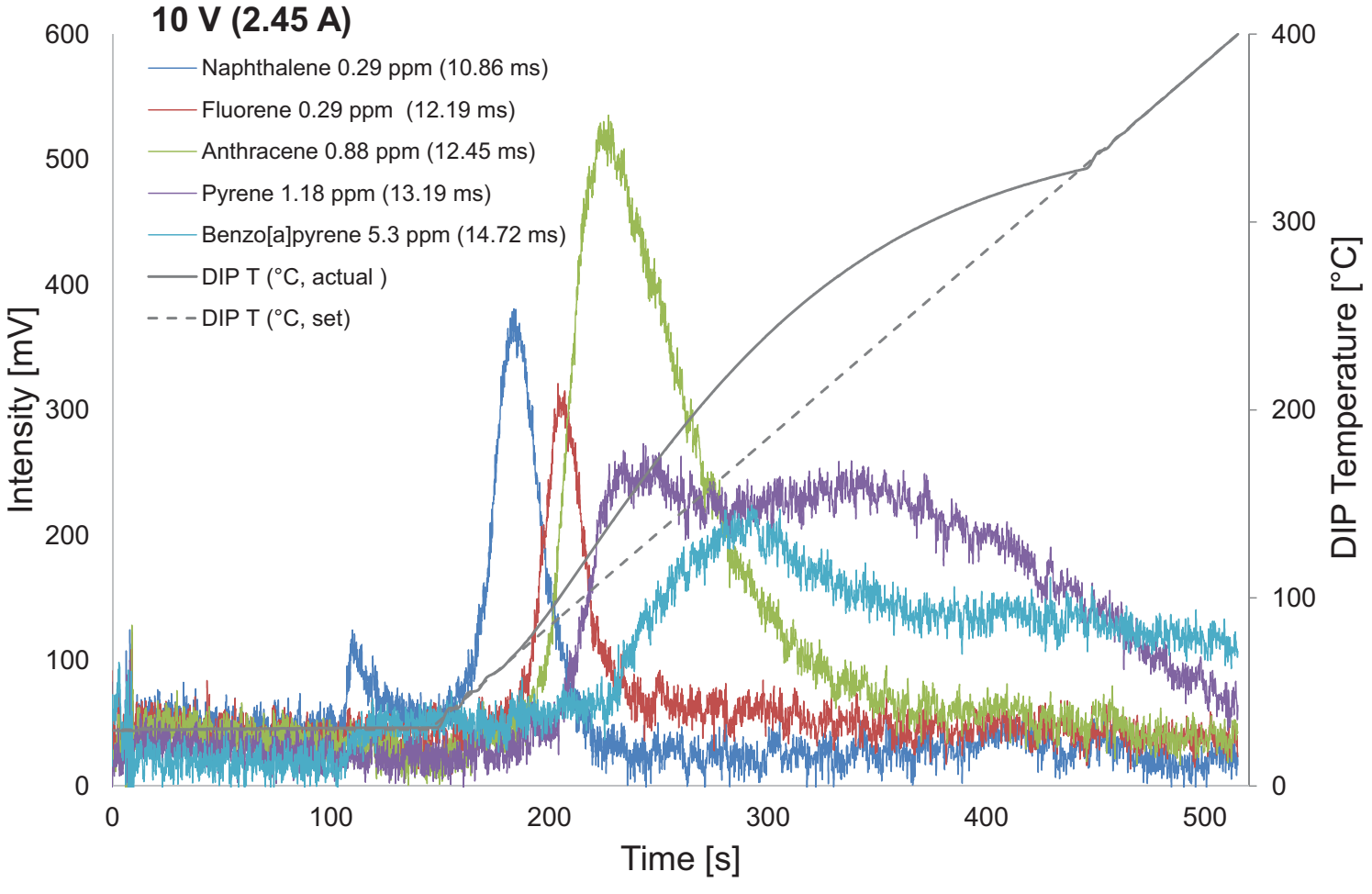

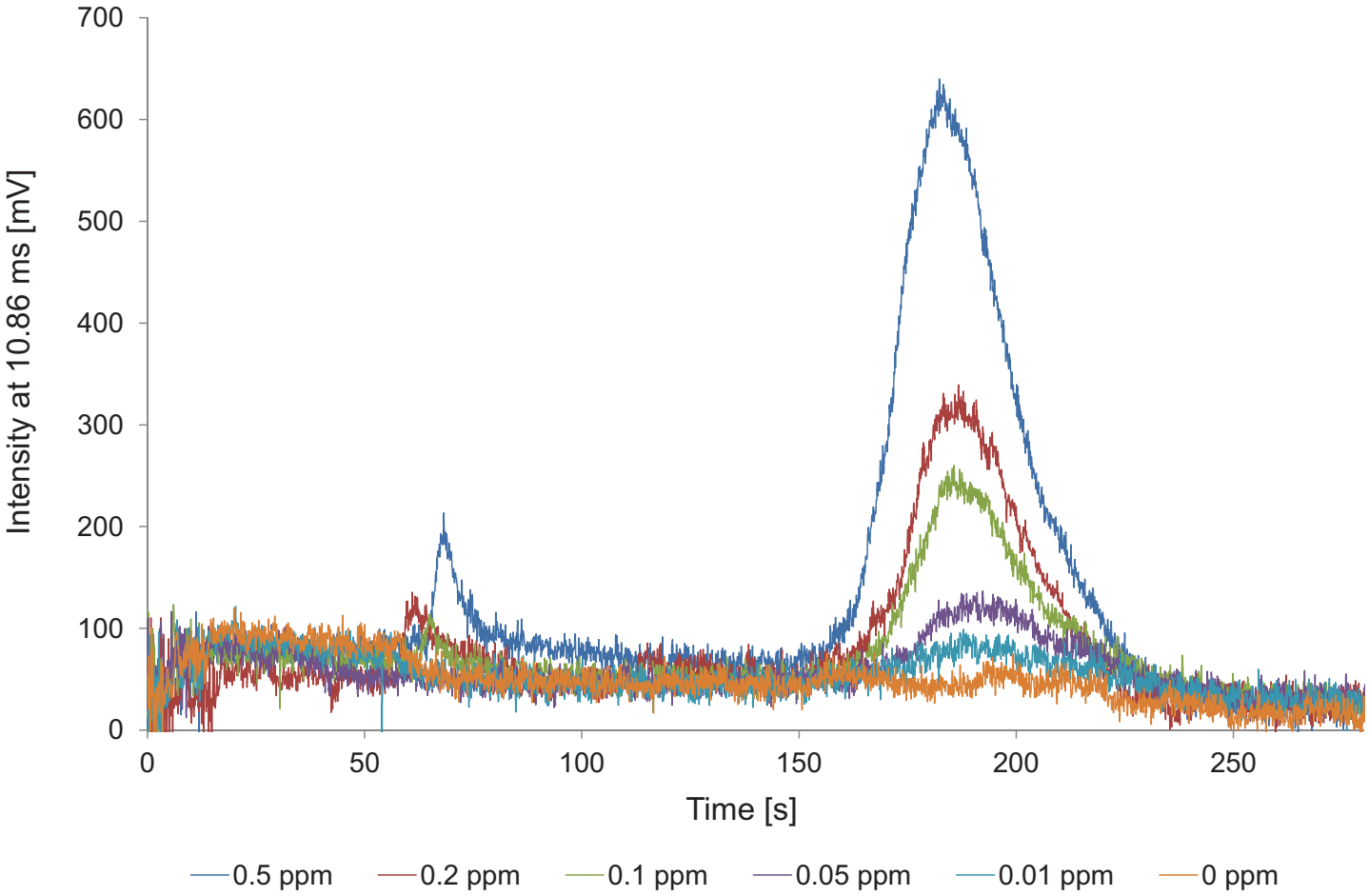
Intensity at 10.86 ms [mV]
700
600
500
400
300
200
100
0
0
50
100
150
200
250
Time [s]
0.5 ppm
0.2 ppm
0.1 ppm
0.05 ppm
0.01 ppm
0 ppm

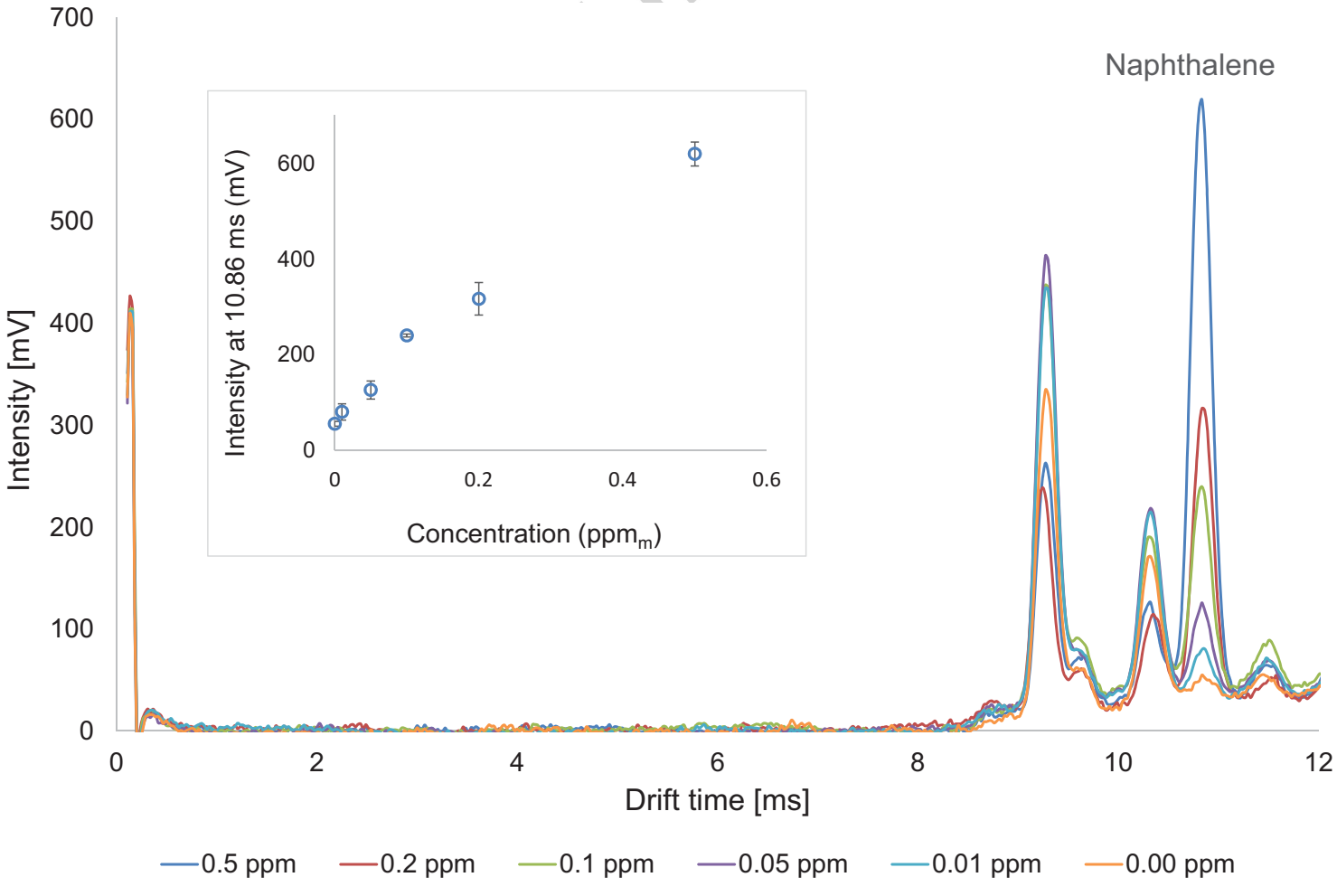
Naphthalene
Intensity [mV]
700
600
500
400
300
200
100
0
0
2
4
6
8
10
12
Drift time [ms]
Intensity at 10.86 ms (mV)
600
400
200
0
0
0.2
0.4
0.6
Concentration (ppm$_m$)
0.5 ppm
0.2 ppm
0.1 ppm
0.05 ppm
0.01 ppm
0.00 ppm

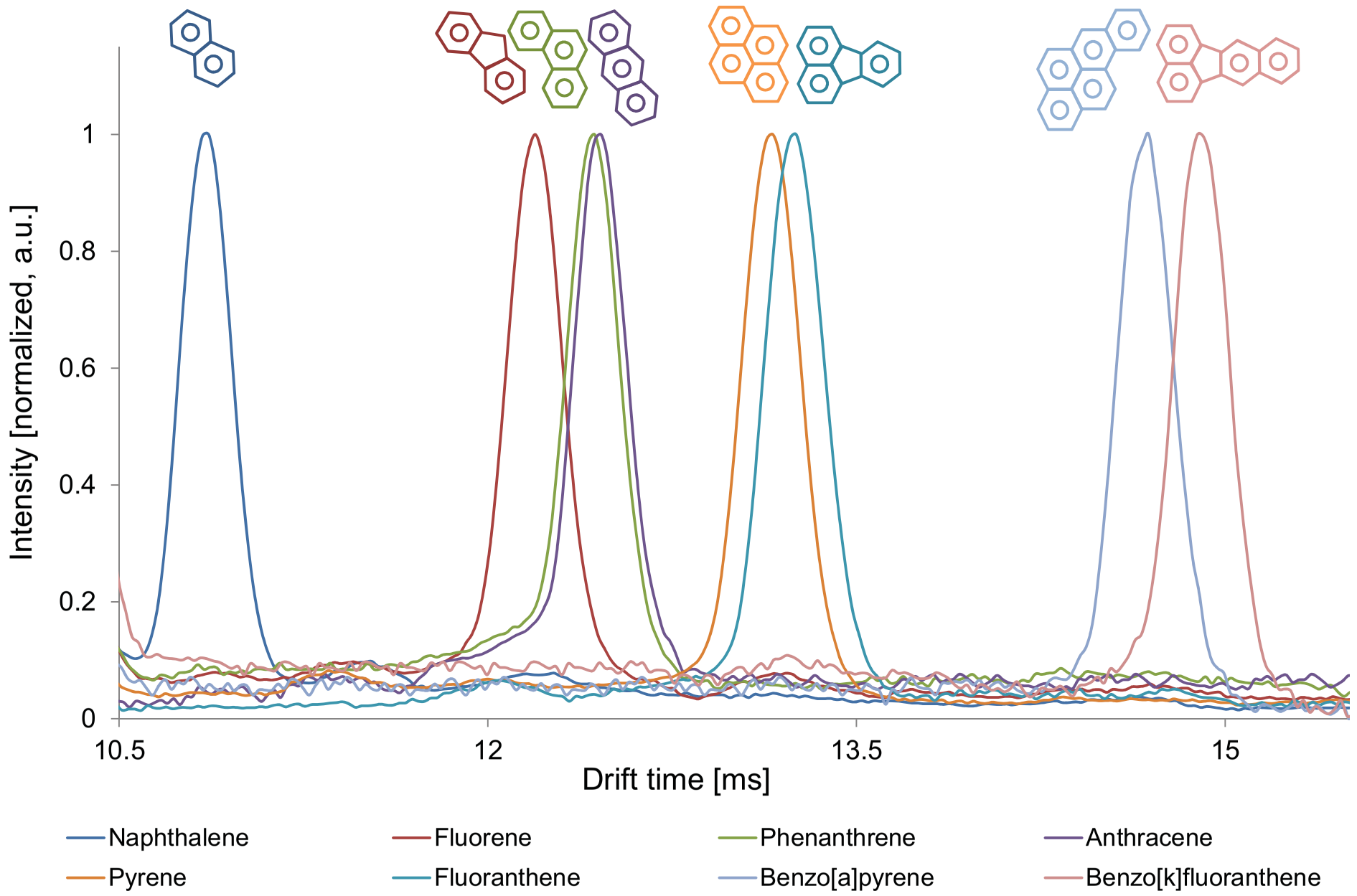

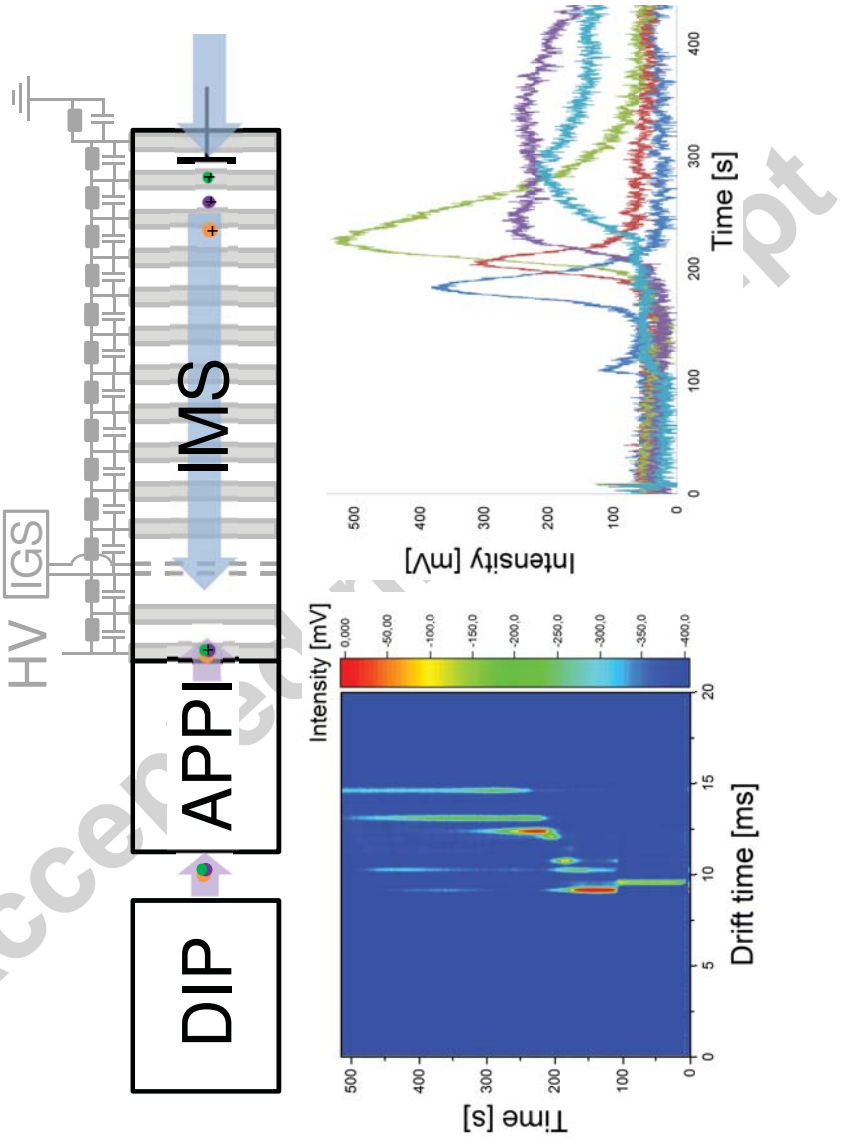

DOI: 10.1016/j.talanta.2017.12.028
URN: urn:nbn:de:hbz:464-20210531-140618-3

Kuklya, Andriy; Coban, Lokman; Uteschil, Florian; Kerpen, Klaus; Telgheder, Ursula (2018). Direct inlet probe ion mobility spectrometry. This is the "Authors Accepted Manuscript" of an article published in: Talanta 180, pages 61-68. Available online 14 December 2017.
The final version may be found at: https://doi.org/10.1016/j.talanta.2017.12.028